

KINEMATIC TIME DEMIGRATION: THE CSP APPROACH

Y. Yang, C. Vanelle, M. Glöckner, and D. Gajewski

email: yan.yang@studium.uni-hamburg.de

keywords: partial time migration, partial time demigration, prestack data regularisation

ABSTRACT

The imaging of low quality data is a challenge in seismic processing. In order to improve the prestack data quality, we suggest a new method of cascaded partial time migration and demigration. The latter is based on a single square root equation in terms of midpoint displacement, half-offset, and migration velocity. By applying the partial time migration, which is a double square root equation in terms of the same parameters mentioned above, and our new partial time demigration, we can enhance the quality of the original data. The resulting new prestack data can be used as input for improved conventional seismic processing and thus lead to better images. The application to a simple and a complex synthetic data set as well as to field data confirms that it can provide images with higher signal-to-noise (S/N) ratio. Furthermore, it has potential for prestack data regularisation.

INTRODUCTION

Handling low quality seismic data is a processing challenge. The quality of reflection seismic data depends on various issues, such as the topography of the earth's surface, the complexity of the subsurface, and the technical equipment used in the acquisition stage. Natural and anthropogenic factors can also affect seismic measurements. Inhomogeneities in the subsurface, the presence of fault structures, and strong velocity contrasts, in, e.g., areas with salt plugs, lead to a decrease of signal-to-noise (S/N) ratio of the data (see, e.g., Baykulov and Gajewski, 2009). These poor quality seismic data cause low quality imaging results. Another issue can arise from an irregular acquisition if methods are applied that require regular data. In order to address these issues, we suggest a method of cascaded partial time migration and demigration.

Hubral et al. (1996) proposed a unified approach to 3D seismic reflection imaging. The approach is composed of

1. *migration*: a weighted Kirchhoff-type diffraction-stack integral to transform (migrate) seismic reflection data from the measurement time domain into the model depth domain,
2. *demigration*: a weighted Kirchhoff-type isochron-stack integral to transform (demigrate) the migrated seismic image from the depth domain back into the time domain.

Although their approach is formulated in the depth domain, the concept can be applied to the time domain. Since processing in the time domain is fast, robust, and less sensitive to velocity model errors, we present according operators. Note that geometric spreading, obliquity, filtering, etc. are not addressed in this work.

Prestack time migration (PreSTM) is a classical tool for subsurface imaging, where the conventional time migration operator is described by a double square root (DSR) equation (see, e.g., Yilmaz, 2001). Furthermore, Dell et al. (2012) suggested the Common Scatter Point (CSP) method, i.e., partial time migration, by re-parametrising the DSR equation in a fashion that preserves the moveout.

In this work, we propose a new operator for partial time demigration, which is the inverse process of partial time migration (e.g., Dell et al., 2012; Yang et al., 2014). The new partial time demigration operator

is based on a single square root equation in terms of midpoint displacement, half-offset, and migration velocity. By applying the partial time migration that is based on a double square root equation in terms of the same parameters mentioned above, we obtain data in a new prestack domain, the CSP domain (Dell et al., 2012). Potential applications for data processing in this domain are diffraction separation and multiple attenuation. In a subsequent step, the new partial time demigration is applied to generate new prestack data in the original domain, however, with an improved signal-to-noise ratio compared to the original data. Furthermore, the proposed method of migration followed by demigration can be used to generate regularised prestack data.

After a brief review of partial time migration, we introduce our new partial time demigration operator. We then verify our method by applying the cascaded migration and demigration to a simple synthetic data set and the complex synthetic Sigsbee 2A data. In order to investigate the performance of the technique, we use previously-determined migration velocities (see Bobsin et al., 2014) as well as root mean square (RMS) velocities that are available in the synthetic case. Furthermore, we apply the method to marine field data. The results confirm the potential of the method.

Another kinematic time demigration method was recently developed by Glöckner et al. (2015). Their technique is based on a different operator, namely, the implicit CRS operator (i-CRS).

METHOD

Partial time migration

The classic 2D time migration operator (e.g., Yilmaz, 2001) describes the diffraction traveltimes t_D by the DSR equation,

$$t_D(t_0, m, h) = \sqrt{\frac{t_0^2}{4} + \frac{(m-h)^2}{v^2}} + \sqrt{\frac{t_0^2}{4} + \frac{(m+h)^2}{v^2}}, \quad (1)$$

where h is half the source-receiver distance, m is the midpoint displacement with respect to the considered CMP position, t_0 is the zero-offset (ZO) two-way traveltime, and v is the migration velocity.

In partial time migration, the DSR operator is parametrised in terms of the apex of the diffraction traveltimes

$$t_{apex} = \sqrt{t_0^2 + \frac{4h^2}{v^2}} \quad (2)$$

for each offset (Dell et al., 2012). Substituting Equation (2) into Equation (1), after some algebra we obtain the partial time migration operator in apex coordinates,

$$t_D(t_{apex}, m, h) = \sqrt{\frac{t_{apex}^2}{4} + \frac{m(m-2h)}{v^2}} + \sqrt{\frac{t_{apex}^2}{4} + \frac{m(m+2h)}{v^2}}. \quad (3)$$

Note that both operators, i.e., classic time migration and partial time migration, provide the same diffraction response. The difference lies only in the parametrisation. The advantage that Equation (3) has over (1) is the preservation of the moveout.

In the partial time migration method, new prestack traces are generated for all midpoints, which constitute the prestack data in the CSP domain. Subsequently, a multi-parameter stack over offsets and midpoints is performed. By thus stacking the data, we achieve the desired prestack data enhancement since the number of contributing traces is much higher than for the single parameter stack over h that is part of classic prestack time migration. Examples for such multi-parameter (MP) stacking operators are the common reflection surface stack (CRS; Müller, 1999), the implicit CRS operator (i-CRS; Vanelle et al., 2010; Schwarz et al., 2014), multifocusing (MF; Gelchinsky et al., 1999), and the shifted hyperbola approach (de Bazelaire, 1988). The output of the MP stack is then, as for the classic time migration, assigned to the point (t_0, m, h) .

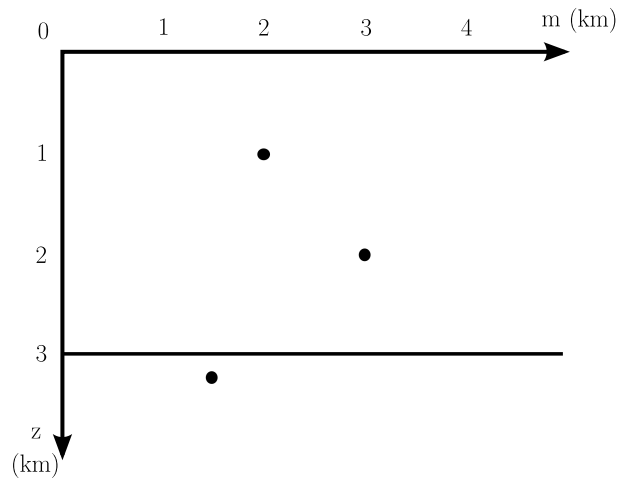


Figure 1: Simple generic synthetic model with three point diffractors and one horizontal reflector.

Partial time demigration

Whereas the migration in the previous step is carried out by stacking the energy along the diffraction operator and assigning the summation result to the corresponding diffraction location, demigration, the inverse process, redistributes the collapsed energy back to each diffraction event in the original time domain.

We achieve this by solving Equation (3) for t_{apex} . After applying again some algebra, we obtain our partial time demigration operator in terms of t_D , which is now the isochron time:

$$t_{apex}(m, h, t_D) = \sqrt{t_D^2 - \frac{4m^2}{v^2} + \frac{(4mh)^2}{v^4 t_{iso}^2}}. \quad (4)$$

Note that the partial time demigration operator is a single square root equation.

If the same parameters, i.e., velocities and apertures, are applied in both steps, partial time migration and partial time demigration, the resulting data are theoretically equivalent to the original data (Hubral et al., 1996). However, due to the data enhancement capability of our method, we obtain a higher signal-to-noise level and thus better image quality. Poststack time-demigrated gathers can be generated by stacking the prestack time-demigrated data.

In the following section, we apply the method to two synthetic data sets and marine field data.

APPLICATIONS

Generic data example

To verify our method, we applied it to a simple synthetic data set that consists of three point diffractors and a horizontal reflector in a homogeneous background (see Figure 1). The data were generated with the Seismic Unix routine *susynlv*. The offset range is 0 to 2 km and the midpoint range is 0 to 2 km with a CMP interval of 12.5 m. A constant velocity of 2 km/s was chosen. The peak frequency of the wavelet used for the modelling is 30 Hz. Furthermore, we added random noise with a signal-to-noise ratio of 5. Figure 2(a) shows the corresponding CMP-stacked section. Note that conflicting dips are present where diffractions and reflections intersect.

In the following tests, we used migration velocities calculated following Bobsin et al. (2014) as shown in Figure 2(b). As expected, the velocity was determined to be 2 km/s in areas where events exist, and undetermined otherwise. For comparison, we also applied our method using the known constant velocity of 2 km/s.

Figures 3(a) and 3(b) show the partially time-migrated and MP-stacked (see Yang et al., 2014) section using the numerical and analytical velocities, respectively. We observe that the diffractions are generally collapsed and the reflector is mapped to the correct position for both velocity models.

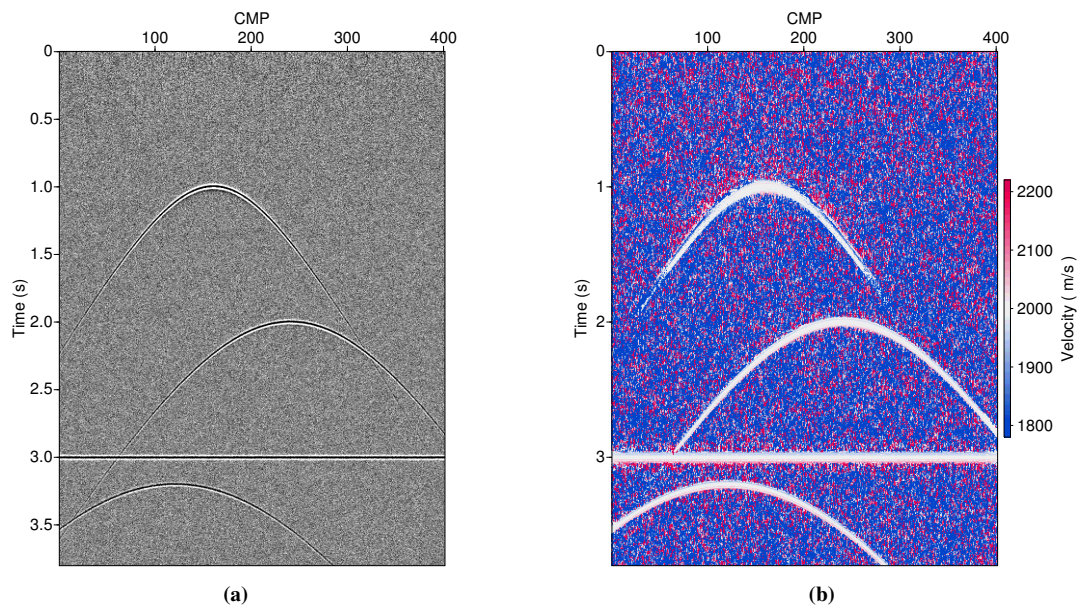


Figure 2: Generic data example: (a) CMP-stack of the original data, (b) velocities determined following Bobsin et al. (2014).

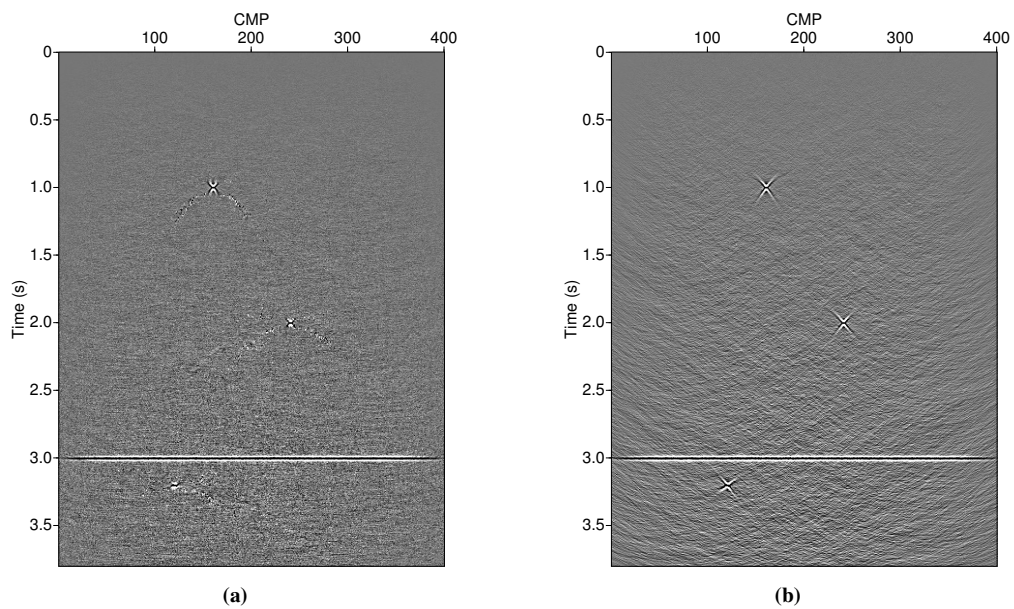


Figure 3: Generic data example: partially time-migrated and stacked result using (a) velocities determined following Bobsin et al. (2014), (b) constant velocity.

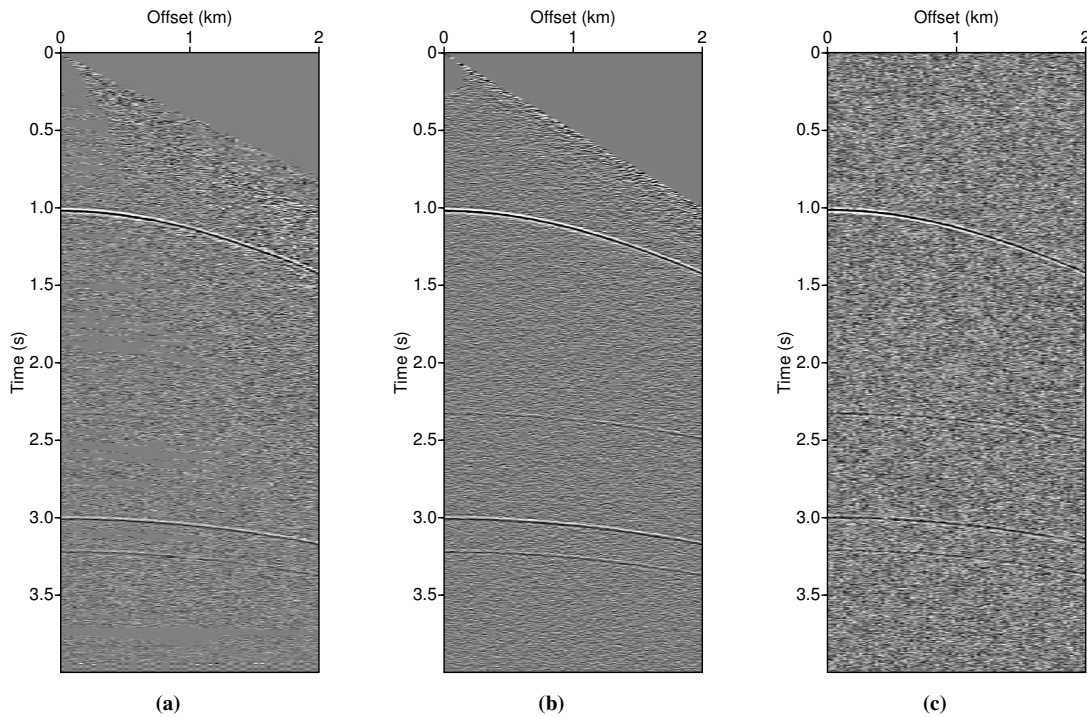


Figure 4: Generic data example: prestack data for CMP 145 obtained from cascaded migration-demigration (a) using velocities determined after Bobsin et al. (2014), (b) using constant velocity. (c) shows the original data for comparison.

The (unstacked) partially time-migrated data were then used as input for the partial time demigration. In Figures 4(a)–(c), we compare the new prestack data resulting from our cascaded migration and demigration for both velocity models with the original data for CMP 145, located at 1.45 km in Figure 1. Both newly-generated gathers show a higher S/N than the original data. The event at 2.3 s was reconstructed with a lower amplitude because the selected CMP position is far from the corresponding diffraction apex. This event was better reconstructed for the constant velocity case.

Finally, Figures 5(a) and 5(b) show the resulting poststack sections of the newly-generated prestack data. Compared with the stacked original data (see Figure 2(a)), we also observe higher S/N. The shorter diffraction tails in the poststack demigration are due to the limited extent of the aperture. Accordingly, choosing larger apertures will result in longer diffraction tails.

Sigsbee 2A data example

To evaluate the performance of our method in a complex setting, we have applied it to the synthetic acoustic Sigsbee 2A data set. It contains a large irregularly-shaped salt body with a rugged top and two lines of point diffractors embedded in the horizontal layering of sediments.

As for the generic model, we applied our new method with migration velocities calculated by Bobsin et al. (2014). Instead of the constant velocity in the previous example, we applied root mean square (RMS) velocities calculated from the interval velocities of the model (see Figure 6) provided by the SMAART JV consortium. Due to the large volume of this data set, we show only the results for an offset of 1 km.

Figures 7(a)–(c) display the 1 km common offset sections resulting from the new method as well as the original data for comparison. We observe that the events were mostly reconstructed except for the complex salt body part, where strong velocity contrasts and triplications exist, which correspondingly degrade the velocity determination. This is particularly the case if velocities from Bobsin et al. (2014) are used. In the result from RMS velocities, we observe an overall better data reconstruction even in the complex salt body part.

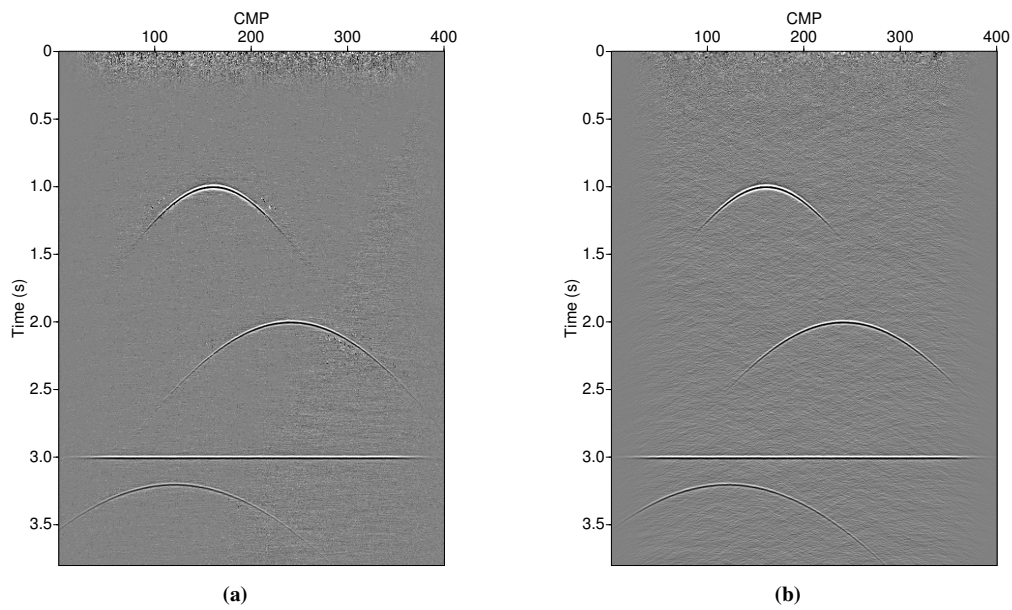


Figure 5: Generic data example: poststack sections of the newly-generated prestack data using (a) velocities determined following Bobsin et al. (2014), (b) constant velocity.

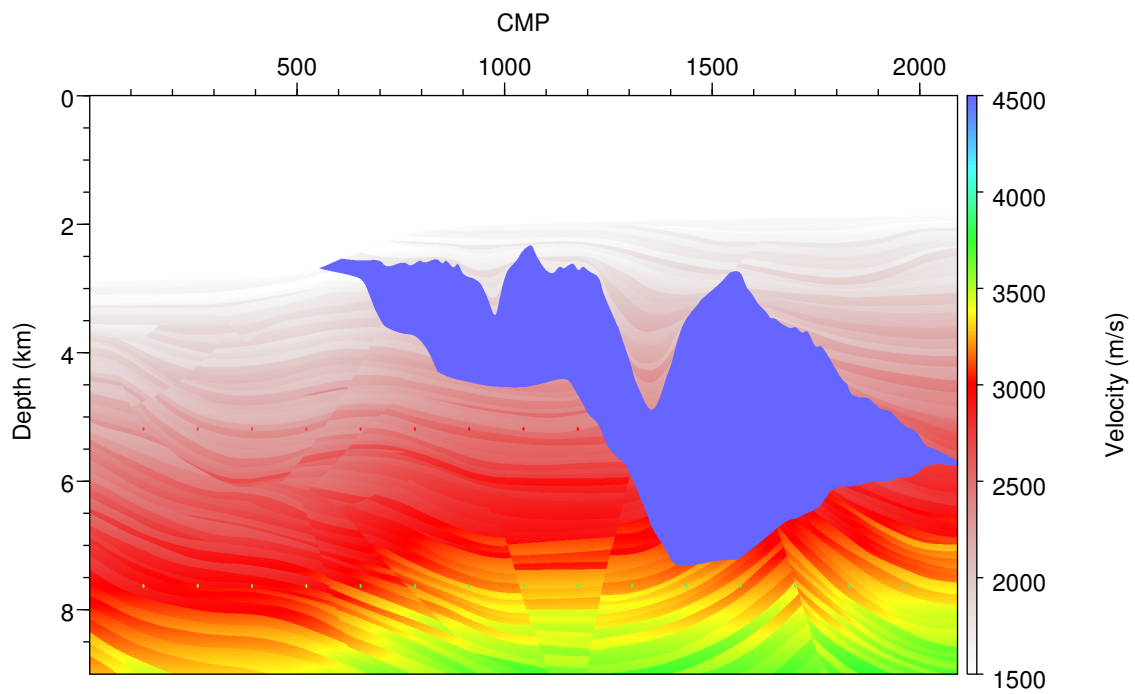


Figure 6: The Sigsbee 2A model.

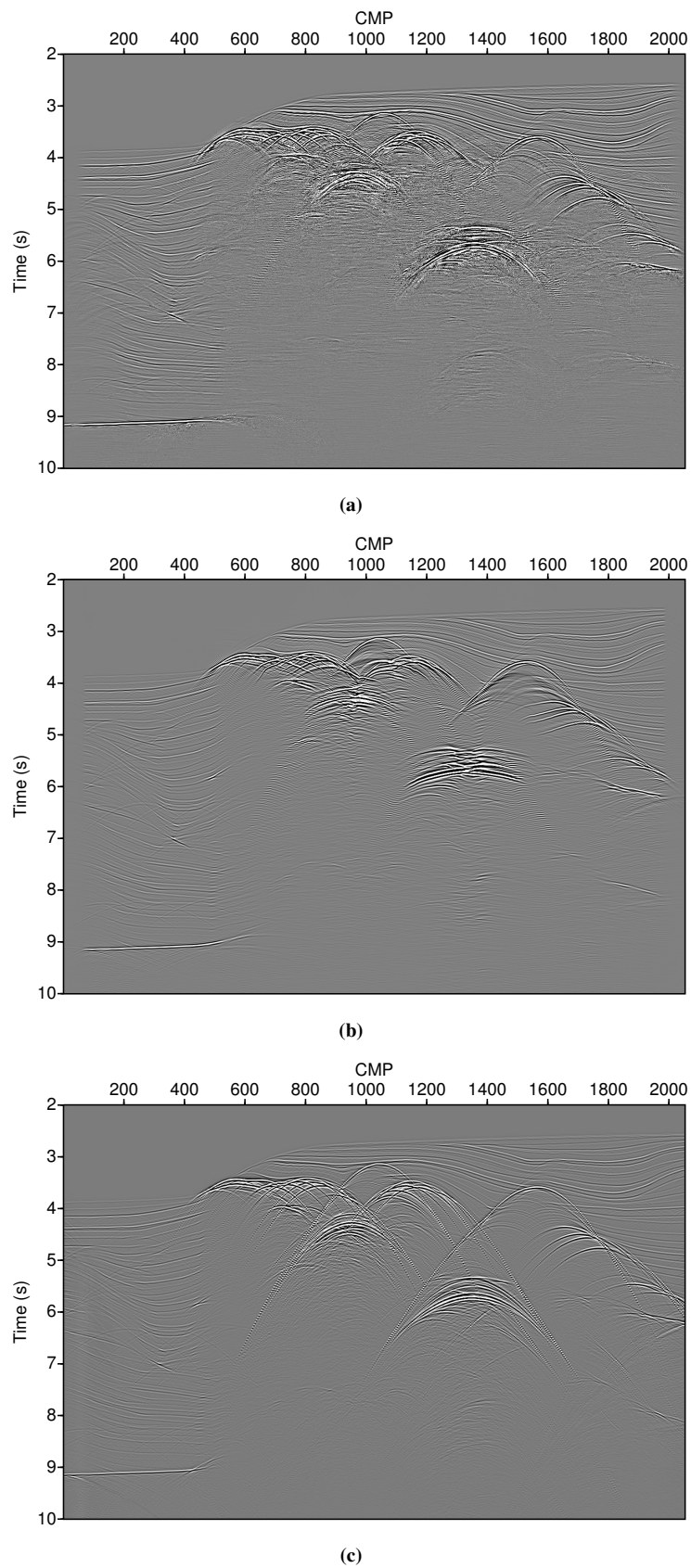


Figure 7: Sigsbee 2A data example: 1 km common offset section for the newly-generated prestack data using (a) velocities calculated by Bobsin et al. (2014), (b) RMS velocities. (c) shows the corresponding original section.

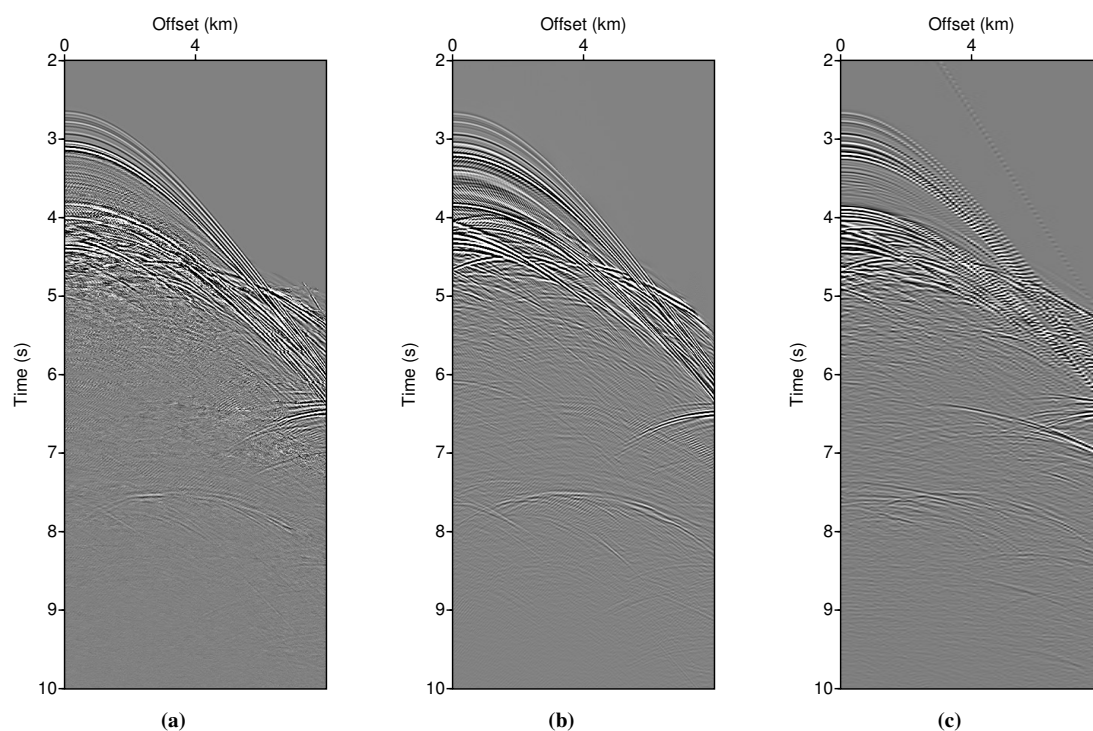


Figure 8: Sigsbee 2A data example: CMP gather 1026 for the newly-generated prestack data using (a) velocities calculated by Bobsin et al. (2014), (b) RMS velocities. (c) shows the corresponding original section.

In Figures 8(a)–(c), we show the new prestack data resulting from the cascaded migration-demigration as well as the original data for CMP 1026. Again, we observe an overall good reconstruction of the data, in particular with RMS velocities.

Furthermore, we show the poststack results in Figures 9(a)–(c). Like in the offset sections in Figures 7 we can observe diffractions and conflicting dips. The conclusions regarding data quality and model dependence are the same as for the reconstructed prestack data.

Marine field data example

Finally, we have applied the method to a marine field data set. The data were acquired in the Levantine Basin in the south-eastern Mediterranean Sea. The Levantine Basin has a complex seismic stratigraphy of the basinal succession. The deformation patterns of the intra-evaporitic sequences include folds and thrust faulting, which gives evidence for extensive salt tectonics and shortening during the depositional phase. Post-depositional gravity gliding caused salt rollers in the extensional marginal domain, compressional folds, and faults within the Levantine basin (Netzeband et al., 2006).

A part of the data consisting of 2000 CMPs covering 15 km was selected for processing. A 2D acquisition with a shot spacing of 25 m and a receiver spacing of 12.5 m was performed. The minimum offset was 150 m, and the maximum offset was 7338 m. The record length is 8 s with a 4 ms sample rate.

We applied our method with migration velocities calculated by Bobsin et al. (2014). Due to the large volume of this data, we present only results for a common offset of 1150 m. Figure 10 shows the offset sections for the newly-generated prestack data and the original data. We observe that the events are reconstructed in the sediments and also in the region with the salt rollers. Figure 11 shows the according poststack sections. They exhibit the same properties as the prestack results.

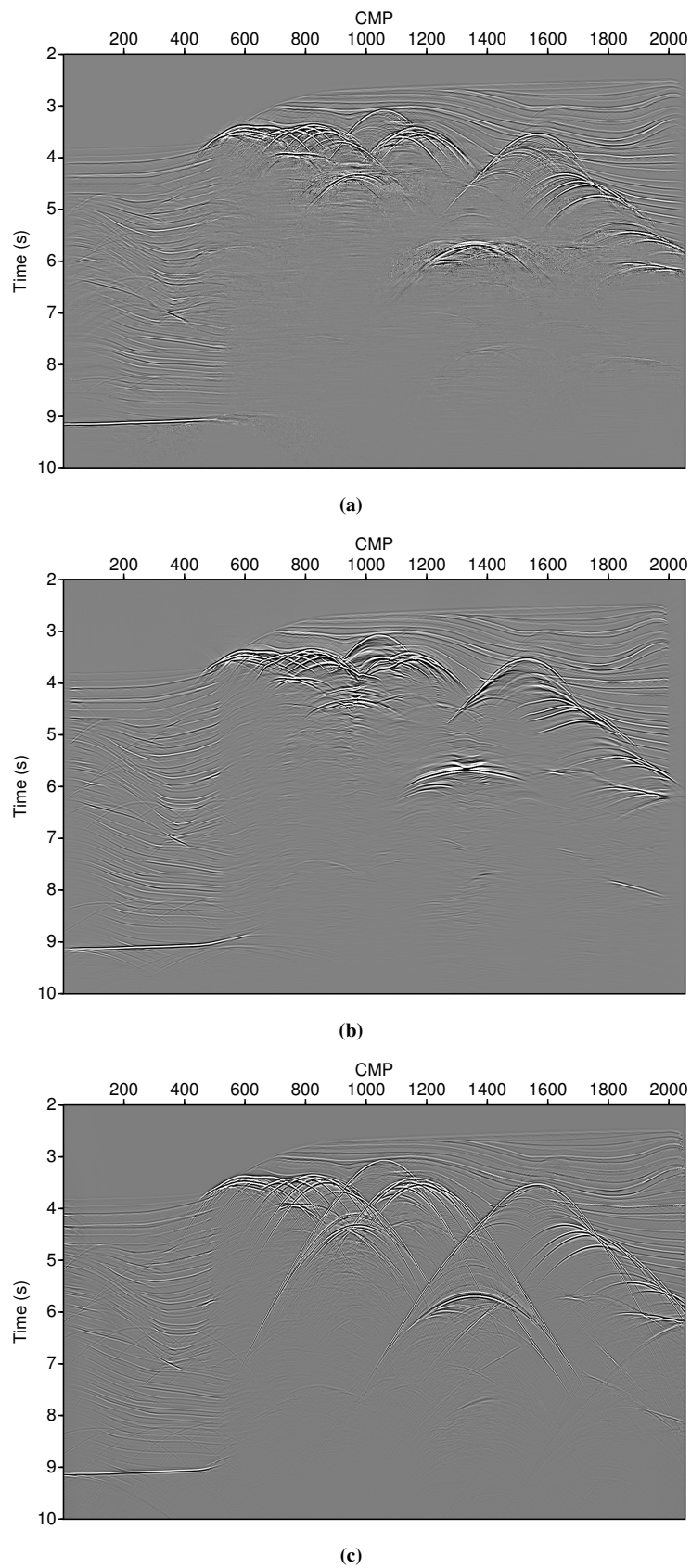
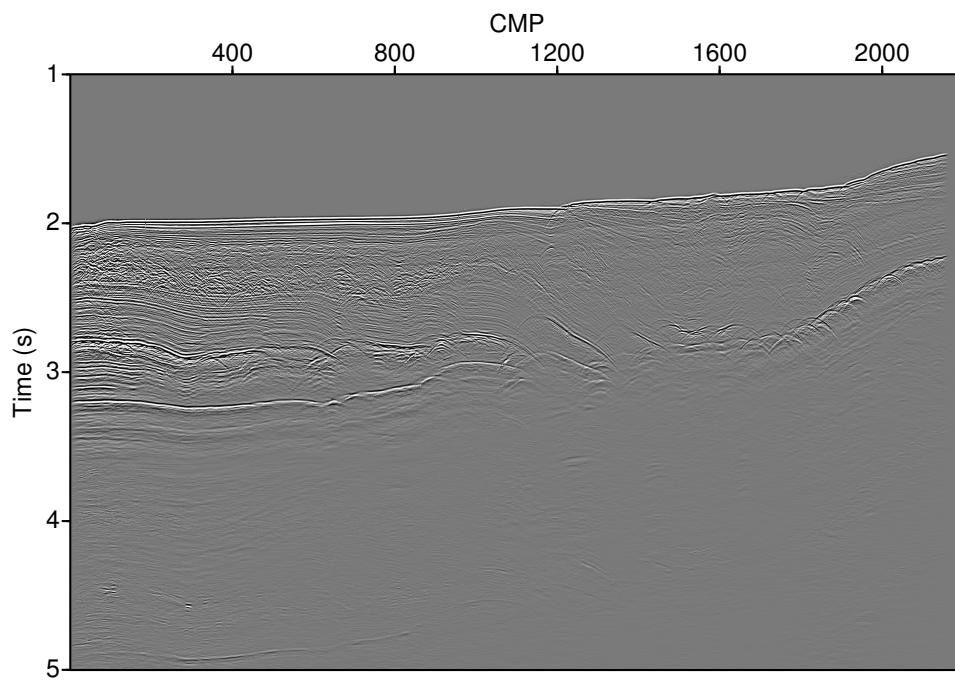
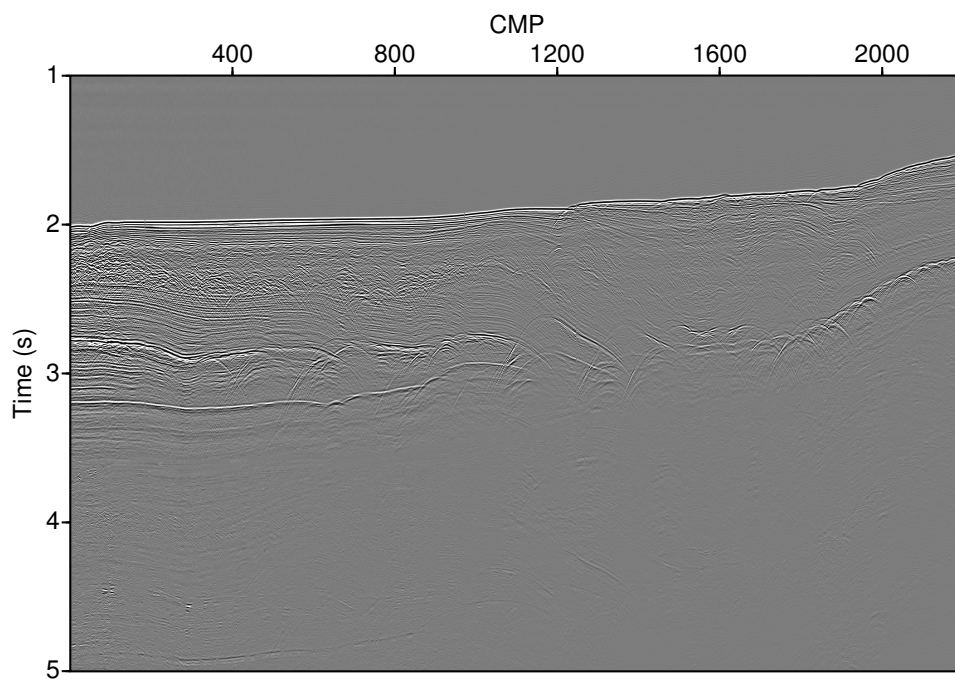


Figure 9: Sigsbee 2A data example: poststack sections of the newly-generated prestack data using (a) velocities determined following Bobsin et al. (2014), (b) RMS velocities. (c) shows the corresponding original section.

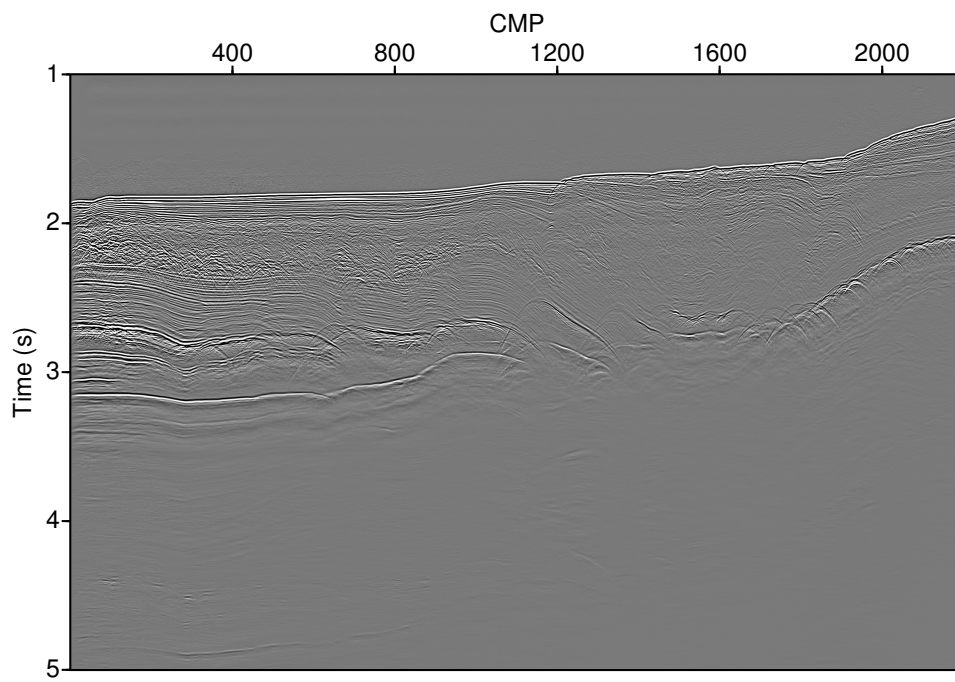


(a)

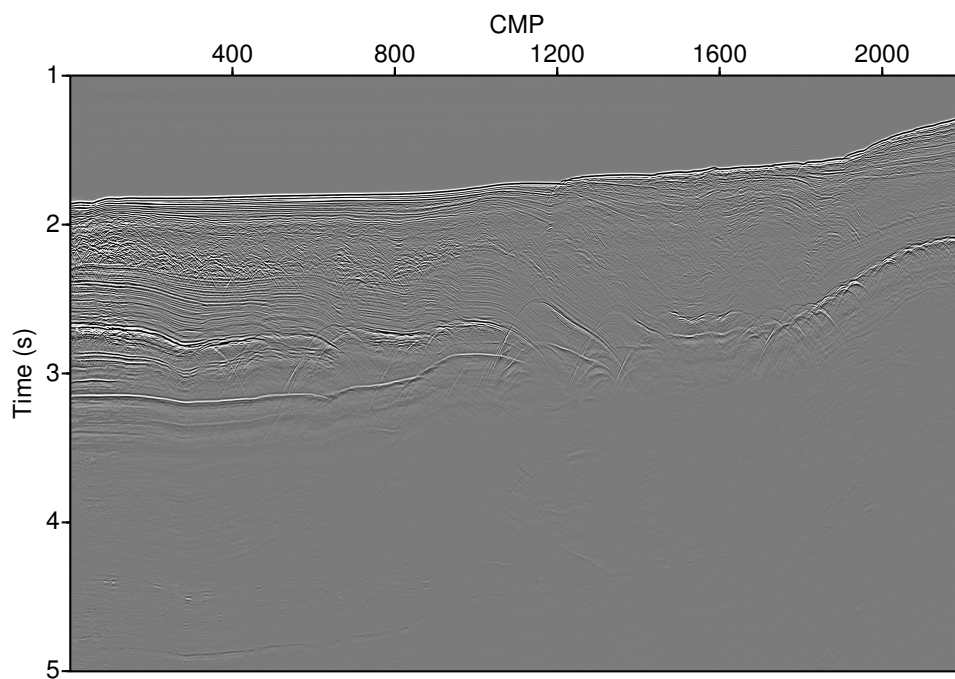


(b)

Figure 10: Marine data example: (a) 1150 m offset section resulting from the new method. (b) shows the corresponding original section.



(a)



(b)

Figure 11: Marine data example: Poststack section of (a) the newly-generated prestack data, (b) the original data.

CONCLUSIONS AND OUTLOOK

We have introduced a new partial time demigration operator. It is expressed by a single square root equation in terms of midpoint displacement, half-offset and migration velocity. Subsequent application of partial time migration and the partial time demigration can enhance the quality of the resulting prestack data compared to the original data. These newly-generated improved prestack data can then be used for further processing. Furthermore, our new method can be utilised for prestack data regularisation.

Application to a simple generic data set as well as the complex synthetic Sigsbee 2A data and field data confirm that the suggested method leads to an improvement of data quality in terms of higher S/N.

Our examples also show that the velocity model is crucial for the quality of the output. Whereas RMS-velocities led to the best results, these are not generally available for field data. In this work, we have used migration velocities obtained from the implicit common reflection surface (i-CRS) operator (see Bobsin et al., 2014). However, these face problems in complex geological situations, e.g. faults or salt bodies. Therefore, an important future step is the improvement of migration velocities.

ACKNOWLEDGEMENTS

We thank the Applied Seismics Group in Hamburg for continuous discussion, in particular Marie Voss for proofreading. We are grateful to the sponsors of the Wave Inversion Technology (WIT) Consortium and the China Scholarship Council (CSC) for technical and financial support. We give our thanks to SMAART JV and TGS for providing the data. Seismic Un*x routines were used for generating the generic data set and displaying the profiles.

REFERENCES

- Baykulov, M. and Gajewski, D. (2009). Prestack seismic data enhancement with partial common-reflection-surface (CRS) stack. *Geophysics*, 74:V49–V58, doi: 10.1190/1.3106182.
- Bobsin, M., Schwarz, B., Vanelle, C., and Gajewski, D. (2014). Time migration applying the i-CRS operator. *Annual WIT Report*, 18:61–69.
- de Bazelaire, E. (1988). Normal moveout revisited – inhomogeneous media and curved interfaces. *Geophysics*, 53:143–157, doi: 10.1190/1.1442449.
- Dell, S., Gajewski, D., and Vanelle, C. (2012). Prestack time migration by common-migrated-reflector-element stacking. *Geophysics*, 77:S73–S82, doi: 10.1190/geo2011–0200.1.
- Gelchinsky, B., Berkovitch, A., and Keydar, S. (1999). Multifocusing homeomorphic imaging – Part 1: Basic concepts and formulas. *Journal of Applied Geophysics*, 42:229–242, doi: 10.1016/S0926–9851(99)00038–5.
- Glöckner, M., Schwarz, B., Vanelle, C., and Gajewski, D. (2015). Kinematic time demigration: the i-CRS approach. *Annual WIT Report*, 19:74–84.
- Hubral, P., Schleicher, J., and Tygel, M. (1996). A unified approach to 3-D seismic reflection imaging, Part I: Basic concepts. *Geophysics*, 61:742–758, doi: 10.1190/1.1444001.
- Müller, T. (1999). *The Common Reflection Surface stack method – seismic imaging without explicit knowledge of the velocity model*. PhD thesis, University of Karlsruhe.
- Netzeband, G., Gohl, K., Hübscher, C., Ben-Avraham, Z., Dehghani, A., Gajewski, D., and Liersch, P. (2006). The Levantine Basin – Crustal structure and origin. *Tectonophysics*, 418:178–188, doi: 10.1016/j.tecto.2006.01.001.
- Schwarz, B., Vanelle, C., Gajewski, D., and Kashtan, B. (2014). Curvatures and inhomogeneities: An improved common-reflection-surface approach. *Geophysics*, 79:S231–S240.
- Vanelle, C., Dell, S., Kashtan, B., and Gajewski, D. (2010). A new stacking operator for curved subsurface structures. In *80th Annual International Meeting, SEG, Expanded Abstracts*, pages 3609–3613, doi: 10.1190/1.3513600.

Yang, Y., Vanelle, C., and Gajewski, D. (2014). Prestack data enhancement by partial time migration: a subsalt case study. *Annual WIT Report*, 18:173–185.

Yilmaz, O. (2001). *Seismic Data Analysis*. SEG Monograph, Tulsa.